Molecular Crystals and Liquid Crystals
Publication details, including instructions for authors and subscription information:
http://www.tandfonline.com/loi/gmcl20

Magnetism in New Classes of TTF-Based Charge Transfer Complexes

Toshiaki Enoki [a], Hisashi Yamazaki [a], Kazuki Okabe [a], Jun-Ichi Nishijo [a], Kengo Enomoto [a], Masaya Enomoto [a] & Akira Miyazaki [a]

[a] Department of Chemistry, Tokyo Institute of Technology, Ookayama, Meguro-ku, Tokyo, 152-8551, Japan

Version of record first published: 18 Oct 2010

To cite this article: Toshiaki Enoki, Hisashi Yamazaki, Kazuki Okabe, Jun-Ichi Nishijo, Kengo Enomoto, Masaya Enomoto & Akira Miyazaki (2003): Magnetism in New Classes of TTF-Based Charge Transfer Complexes, Molecular Crystals and Liquid Crystals, 379:1, 131-140

To link to this article: http://dx.doi.org/10.1080/713738655

Mol. Cryst. Liq. Cryst., Vol. 379, pp. 131-140

1058-725X/02 $12.00 + .00
DOI: 10.1080/10587250290090372

Magnetism in New Classes of TTF-Based Charge Transfer Complexes

TOSHIAKI ENOKI, HISASHI YAMAZAKI, KAZUKI OKABE, JUN-ICHI NISHIJO, KENGO ENOMOTO, MASAYA ENOMOTO and AKIRA MIYAZAKI

Department of Chemistry, Tokyo Institute of Technology, Ookayama, Meguro-ku, Tokyo 152-8551, Japan

Charge transfer (CT) complexes are promising for developing molecule-based magnets, where π-electrons play an important role. New classes of molecular magnets are presented in the TTF-based CT complexes from points of unconventional magnetism. π-d interaction in d-electron-spin-incorporated CT complexes give anomalous effect of magnetic transition on the electron transport. The coexistence of metallic conduction and localized spin feature appears in the system located in the metal-insulator boundary. 1D metal having ferromagnetic interaction and triangle-based spin ladder system are also obtained from CT complexes.

Keywords: organic metal; molecular magnet; π-d interaction; metal-insulator transition; spin ladder; ferromagnet

INTRODUCTION

Charge transfer (CT) complexes provide a fruitful realm in the development of molecular magnets, where low-dimensional (low-D) electronic phases give a large variety of magnetic systems among π-d composite magnets, magnetic conductors, ferromagnetic metals, low-D

magnets, etc. There are two categories in these CT complexes from magnetism aspects; (1) pure π-electron magnetic system, (2) π-d composite magnetic system, where localized d-electron spins are incorporated as ingredients. In the former, low-D quantum spin systems appear in the localized-electron regime, where the electron correlation overwhelms the kinetic energy. In the metal-insulator (MI) boundary, highly correlated electrons show spin/charge separation. In the conducting π-d systems, the interaction between conduction π-electron and localized d-spin gives metal magnets. In the insulating systems, the coexistence of π- and d-spins brings about ferrimagnets, weak ferromagnets, and some other unconventional magnets. We discuss the properties of TTF-based magnetic complexes we have developed under the impetus mentioned above. Figure 1 shows the list of TTF-type donors employed in the present work.

π-d INTERACTION SYSTEMS

$(DMET)_2FeBr_4$, $(EDTDM)_2FeBr_4$ and $(EDS\text{-}TTF)_2FeBr_4$ are isostructural to each other, as shown in Figure 2[1-3]. They consist of alternate stacking of donor conducting sheets and square lattice magnetic sheets of Fe^{3+} localized spins (S=5/2) along the *c*-axis. In each

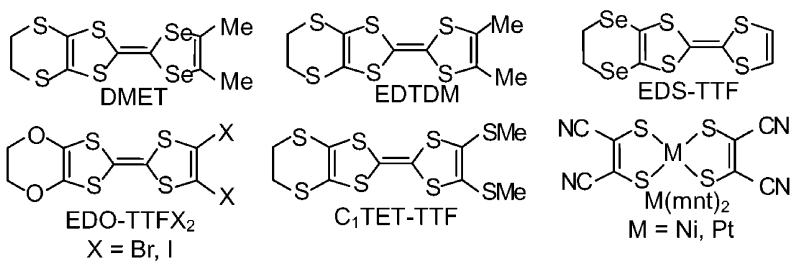

FIGURE 1. Molecular structures of the donors and acceptors.

donor sheet, donors form a 3/4 filled quasi-1D π-electronic system. The resistivity behaves metallic down to T_{MI}~40 and 15K for $(DMET)_2FeBr_4$ and $(EDTDM)_2FeBr_4$, respectively, below which insulating SDW state emerges. $(EDS\text{-}TTF)_2FeBr_4$ behaves semiconductive below T_{MI} ~ 250K.

The magnetism is governed mainly by Fe^{3+} localized spins. In the DMET and EDTDM systems, Fe^{3+} spins undergo 3D antiferromagnetic (AF) ordering at T_N=3.7 and 3K, respectively, below which the spin easy axis is oriented to the *a*-axis. No magnetic transition occurs in $(EDS\text{-}TTF)_2FeBr_4$, in contrast to other two counterparts. Magnetization curves behave anomalously, as shown in Figure 3(a). Applying the field along the *a*-axis gives a spin flop transition at B_{sf}~2T and 1.8T for the DMET and EDTDM cases, respectively. However, the linear part of the

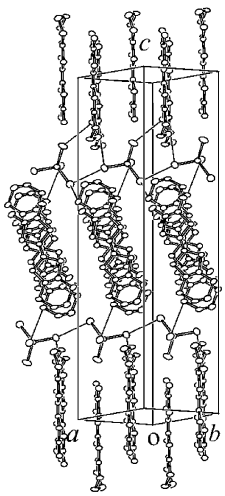

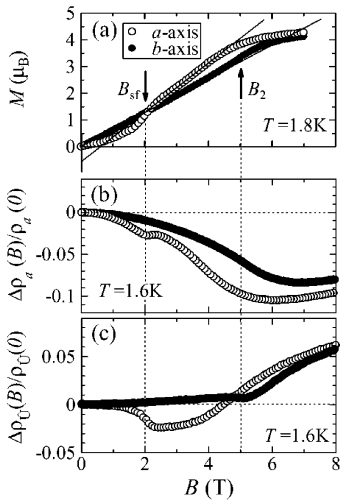

FIGURE 2.(left) Structure of D_2FeBr_4 (D=DMET, EDTDM, EDS-TTF). Solid lines: close intermolecular contacts.

FIGURE 3.(right) Temperature dependence of the magnetization (a), in-plane magnetoresistance (b), and inter-plane magnetoresistance (c) for $(DMET)_2FeBr_4$.

magnetization curve above B_{sf} is not extrapolated to the origin, different from the behavior of ordinary AF magnets. For the hard axis direction (*b*-axis), an anomaly appears around B_2~5T. These magnetization features cannot be explained only by Fe^{3+} spins. In other words, donor electrons participate in the magnetism, modifying the features from those of ordinary AF magnets.

Figures 3(b) and (c) represent the magnetoresistance (MR) vs field plot below T_N for $(DMET)_2FeBr_4$. For the in-plane transport, the MR is negative in the whole field range up to 15T with a minimum appearing around 6T. Interestingly, an anomalous discontinuity exists at B_{sf} for the easy axis direction. In contrast, the inter-plane MR is negative only up to ca. 5T with a spin-flop-induced singularity in the easy axis direction, while the MR becomes positive above that field. For the hard axis direction, the MR is positive with a discontinuous change at B_2~5T, at which the magnetization has an anomaly.

The correlation between the magnetic behavior and the MR features can be understood on the basis of the formation of SDW in the insulating phase. Below T_{MI}, localized spins generated in the donor system are spatially ordered. Simple consideration gives the four-fold periodicity in the SDW state along the donor chain, since the electronic state is featured with the 3/4 filled state. In the SDW state, Fe^{3+} spins become antiferromagnetically ordered below T_N, where the periodicity of the Fe^{3+} AF arrangement is well registered to the SDW with a stabilization energy, making the SDW translational motion destabilize the magnetic energy. However, well above the field at which all the Fe^{3+} spins are ferromagnetically arranged, no energy is required in the SDW translational motion. Therefore, the elevation of the field gives

negative MR up to the saturation field of Fe^{3+} spins. At fields higher than the field at which SDW state is destroyed, individual electrons contribute to the transport, making an upturn of the MR. The anomaly at B_{sf} in the MR is the consequence of a subtle change in the magnetic energy, which affects the SDW translational motion.

ORGANIC METAL WITH FERROMAGNETIC INTERACTION

(EDO-$TTFI_2$)$M(mnt)_2$ (M=Ni, Pt) are featured with a combination of 1D metal of donor EDO-$TTFI_2$ columns and 1D magnetic chains of $M(mnt)_2$ anion columns, which are aligned in parallel to each other along the *c*-axis, as shown in Figure 4[4]. The donor chain forming 3/4 filled state takes an MI transition at T_{MI}=88 and 96K for M=Ni and Pt, respectively. The anion is in the half-filled state with localized spin of S=1/2. The susceptibility vs temperature plot is shown in Figure 5. It evidences the presence of ferromagnetic interaction as clearly seen from the increasing trend of χT at low temperatures for M=Ni and Pt. Actually, the observed susceptibility can be well explained in terms of the S=1/2 1D Heisenberg ferromagnet model with J=18K for M=Ni, taking into account the isotropic susceptibility as shown in Figure 5(a). The absence of 3D long range order is the consequence of 1D Heisenberg isotropic spin feature. In the Pt complex, the susceptibility has a large anisotropy depending on the field directions as shown in

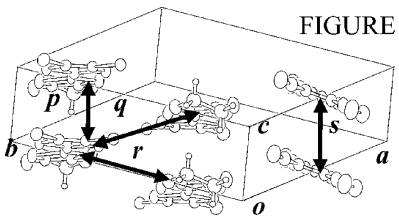

FIGURE 4. Crystal structure of (EDO-$TTFI_2$)$_2$M$(mnt)_2$ (M=Ni, Pt). Arrows correspond to the transfer integrals; intra-donor chain *p*, inter-donor chain *q*, *r*. intra-anion chain *s*.

Figure 5(b), where the fitting is satisfactory with the S=1/2 1D Ising ferromagnet model with J=22K. A 3D long range ordering takes place at T_N=5.5K, where the weak inter-chain AF interaction plays an important role with the aid of the anisotropy, giving an antiparallel arrangement of ferromagnetic chains.

The origin of the ferromagnetic interaction can be explained in terms of McConnel's theory[5]. The spin polarization effect causes ferromagnetic interaction. The slipped metal-over-sulfur configuration of $M(mnt)_2$ molecules gives AF interaction between the small negative spin density on the sulfur atom of an $M(mnt)_2$ and the large positive spin density on the metal atom of adjacent $M(mnt)_2$. Eventually, this local AF configuration produces the ferromagnetic interaction between the metal atoms of adjacent $M(mnt)_2$ molecules.

The interaction between π-carriers and localized spins is an important issue in the development of molecular metal magnets. From this viewpoint, the ESR signal featured with a single Lorentzian for M=Ni and the absence of ESR signal for M=Pt indicate the presence of considerable interaction between donors and magnetic anions.

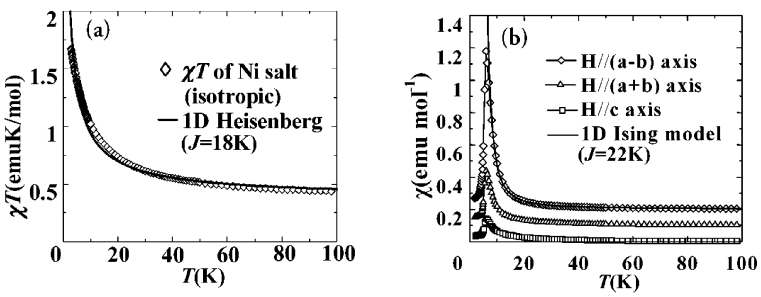

FIGURE 5. (a) χT vs T plot for $(EDO\text{-}TTFI_2)_2Ni(mnt)_2$. (b) χ vs T plot for $(EDO\text{-}TTFI_2)_2Pt(mnt)_2$. The data for $H//(a+b)$ and $(a\text{-}b)$ are shifted up by 0.1 and 0.2, respectively, for clarify.

MAGNETIC CONDUCTOR IN THE MI BOUNDARY

The structure of $(EDO\text{-}TTFBr_2)_3I_3$ is characterized with 1D donor columns in the *a*+*c* direction, as shown in Figure 6. The donors form 2D layers in the *ac*-plane, which are sandwiched between I_3^- layers. Tight-binding band calculation suggests a quasi-1D metallic nature with the presence of a Fermi surface. The conductivity behaves consistently with the predicted band structure in part. The resistivity with $\rho_{rt}\sim 10^{-2}\,\Omega$cm decreases as the temperature is lowered down to about 150K, proving metallic state, and then it shows a semiconductive upsurge below the temperature after the onset of an MI transition at $T_{MI}\sim$150K. The magnetic properties are apparently inconsistent with the electron transport properties. Figure 7 shows the susceptibility vs temperature plot. The susceptibility increases as the temperature is lowered down to ca. 70K, and then it shows a steep decrease after a broad maximum around 70K. It takes a discontinuous change at 15K, below which it increases. Interestingly, no discontinuous change is observed in the susceptibility at the MI transition. The susceptibility

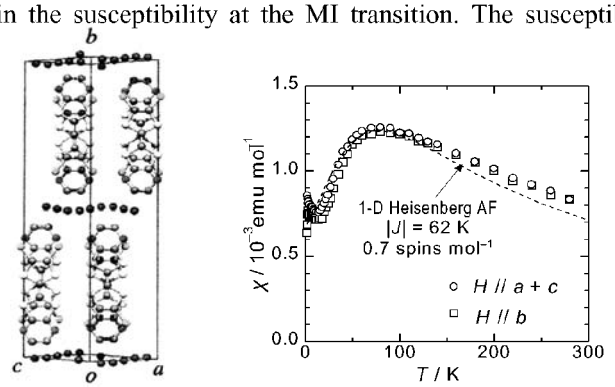

FIGURE 6(left). Crystal structure of $(EDO\text{-}TTFBr_2)_3I_3$.
FIGURE 7(right). The susceptibility vs temperature plot for $(EDO\text{-}TTFBr_2)_3I_3$.

behavior above 15K is reminiscent of that expected for 1D Heisenberg AF system of localized spins, which seems inconsistent with the metallic feature with conduction carriers. Fitting with the 1D AF model AF model gives estimates of exchange interaction $|J|$~62K and the localized spin concentration of 0.23 spin/donor. Moreover, there is a deviation from the model at high temperatures, which is pronounced as the temperature is elevated. This suggests inappropriateness of the fitting with the 1D AF Heisenberg model in the high temperature at least above ca. 150K. The estimated spin concentration is less than that expected from the anion donor composition ratio (1/3). The apparent small localized spin concentration is associated with a fractional value of a localized spin, which might come from a trace of itinerant feature of the electron in the MI boundary. Eventually, the system is featured with a 1D AF localized spin system, whereas the electron transport is explained in terms of metallic conduction carriers. The coexistence of metallic feature and localized spins is not compatible according to the conventional theory of electrons. The enhanced deviation of the susceptibility from that expected from the 1D Heisenberg model above ca. 150K proves that the metallic feature is pronounced at the expense of the localized spin feature in that temperature range.

The discontinuous change in the susceptibility at T_N=15K is associated with the onset of an AF transition.

π-ELECTRON-MEDIATED SPIN LADDER MAGNETS

Donor π-electrons are useful building blocks in constructing superexchange network between localized spins. From this aspect,

(C_1TET-TTF)FeX_4 (X=Cl, Br) are interesting examples in giving a spin ladder system[6]. They are composed of Fe^{3+} zigzag chains and donor dimers. The direct X-X and X-donor-X contacts work to give superexchange paths J_1 and J_2, respectively, resulting in the formation of triangle-based spin-ladder system where J_1 and J_2 correspond to the rung and leg of a ladder, as shown in Figure 8.

For X=Br, the susceptibility shows an AF transition at T_N=4.2K, where the easy axis becomes oriented along the a^*-axis. The peak at T_N, which is accompanied by field dependent susceptibility behavior in the b-axis direction, suggests weak ferromagnetism. The weak ferromagnetic feature is clearly seen in the magnetization shown in Figure 9. The magnetization curve has a spin-flop transition at H_{sf}=2.3T in the a^*-axis direction, while the b-axis magnetization gives an additional magnetization above H_{wf}=2.3T. The weak ferromagnetism is considered to come from spin canting. For X=Cl, ordinary AF transition takes place at T_N=2.5K, below which the easy axis is tilted by

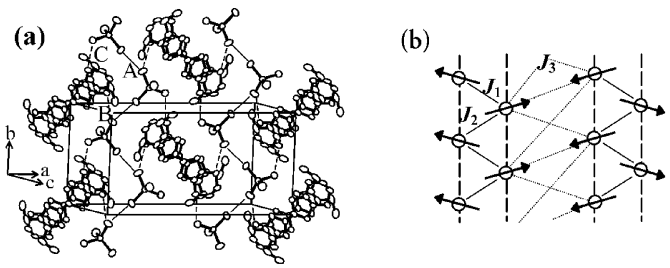

FIGURE 8 (a) The structure of (C_1TET-TTF)FeX_4 (X=Cl, Br), with close contacts between two X atoms (A) of adjacent FeX_4^- anions and those of X-S atoms (B, C) between FeX_4^- and C_1TET-TTF donor. (b) The schematic model of exchange path network for triangle-based spin ladder system. J_1, J_2 and J_3 correspond to Fe-X-X-Fe, Fe-X-D-X-Fe and Fe-X-$(D)_2$-X-Fe, respectively, where D denotes donor.

45° with respect to the *a**-axis in the *ac*-plane.

The feature of triangle-based spin ladder appears in the ordered state. (C_1TET-TTF)FeX_4 (X=Cl, Br) take AF ground state in the ordered phase although the spin canting exists for X=Br. Molecular field treatment gives estimates of the J_2/J_1 ratio at 0.28 and 0.20 for X=Br and Cl, respectively. According to theory of classical triangle-based spin ladder[7], a collinear AF state is stabilized for $J_1/J_2<0.25$, while a spiral state appears above that ratio. This suggests apparent inconsistency in the case of X=Br. The inter-ladder interaction J_3 ($\sim 6\times10^{-3} J_1$) is found to be crucial in stabilizing the AF state from calculation.

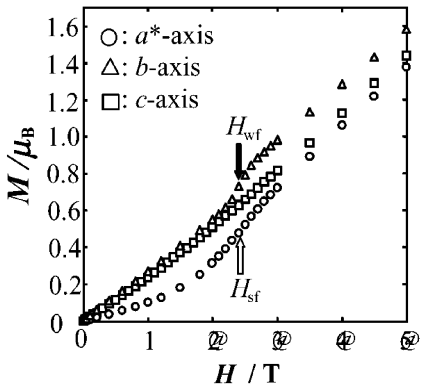

FIGURE 9. The magnetization curves of (C_1TET-TTF)$FeBr_4$ at 2K.

References

[1.] K. Enomoto, A. Miyazaki, and T. Enoki, *Synth. Metals*, **120**, 977 (2001).
[2.] K. Okabe, K. Enomoto, A. Miyazaki, and T. Enoki, *Mol. Cryst. Liq. Cryst.*, to be published, (2001).
[3.] A. Miyazaki and T. Enoki, *Synth. Metals*, to be published, (2002).
[4.] J. Nishijo, E. Ogura, J. Yamaura, A. Miyazaki, T. Enoki, T. Takano, Y. Kuwatani, and M. Iyoda, *Solid State Commun.*, **116**, 661 (2000).
[5.] H. M. McConnel, J. Chem. Phys., 39, 1910 (1963).
[6.] M. Enomoto, A. Miyazaki, and T. Enoki, *Bull. Chem. Soc. Jpn.*, **74**, 459 (2001).
[7.] S. Pati, R. Chitra, D. Sen, S. Ramasesha, and H. R. Krishnamurthy, *J. Phys.: Condens. Matter.*, **9**, 219 (1997).